A Modeling Approach Based on Laminated Plate Theory to Design Microbeams

S. C. Mantell, E. Longmire, and D. Wolters

University of Minnesota, Minneapolis, MN, USA, smantell@me.umn.edu

ABSTRACT

MEMs microbeams consist of many thin material layers. This thin layered structure is very similar to that of laminated composite plates in which thin layers of fiber-reinforced plastic are stacked and cured. Both the MEMs layered structure and the composites layered structure will have layers with different mechanical properties. Researchers in composite materials have developed an approach, referred to as laminated plate theory, to solve mechanics problems in these layered structures. This approach can be extended to characterizing MEMs mechanical behavior. For example, laminated plate theory can be used to evaluate displacement of MEMs microbeams that are actuated by PZT. In this work, measured deflections for a 1000 μm long, 300 μm wide, 2.675 μm thick beam are compared to laminated plate theory predictions. The model accurately predicts the deflection as a function of voltage applied to the PZT. An application of laminated plate theory to prediction of residual stresses is also briefly discussed.

Keywords: microbeams, plate theory, deflection, PZT actuation

1 INTRODUCTION

Analysis of the mechanical performance of MEMS is key to designing and evaluating these structures. It is desirable to predict the structure deflection and stresses that result from external mechanical and thermal loads. For example, deflection resulting from an input voltage is a common performance measure for PZT actuated structures. Both analytic and numerical approaches have been employed in predicting mechanical performance of MEMS [1; 2]. These modeling efforts have focused on thermal loads (residual stresses and strains), PZT actuation, and response to magnetic fields. The one common feature of all the methods is the layered MEMS structure in which each layer has a unique set of mechanical properties. Classical laminated plate theory (CLPT) is an analytic approach that has been extensively applied to mechanical performance of layered, fiber-reinforced composite materials [3]. Just as in MEMS structures, composite materials are comprised of individual layers, each with a unique set of properties. Common loads in composite structures include mechanical loading, such as tension/compression and bending, and thermal loads. In CLPT, the individual layer properties are combined to create an overall matrix of laminated properties. Predicting structure (laminate) response to external loads (either imposed forces/moments or strains/curvatures) is reduced to solving a system of matrix equations. This methodology can be easily applied to MEMS "laminate" structures.

2 THEORY

In the most general form of CLPT, anisotropic material properties for each layer are allowed. Two sets of coordinates are required: a local coordinate system (1, 2, 3) to describe the mechanical behavior at the layer and a global coordinate system (x, y, z) to describe the behavior of the laminate (Figure 1). The formulation is simplified to consider plane stress cases (i.e. stresses in the z direction are much smaller than those in the x-y plane). The most common application of CLPT is to composite materials, in which layer properties are orthotropic (i.e. having three mutually perpendicular planes of material symmetry). Following these assumptions, the stress strain relationship for each orthotropic layer follows a two dimensional Hooke's law approximation:

$$\begin{Bmatrix} \sigma_1 \\ \sigma_2 \\ \tau_{12} \end{Bmatrix} = \begin{bmatrix} Q_{11} & Q_{12} & 0 \\ Q_{12} & Q_{22} & 0 \\ 0 & 0 & Q_{66} \end{bmatrix} \begin{Bmatrix} \varepsilon_1 \\ \varepsilon_2 \\ \gamma_{12} \end{Bmatrix} \quad (1)$$

The symbols σ and ε refer to the stresses and strains in the 1-2 plane (Figure 1), where the 1-2 plane is aligned with the axes of symmetry in the individual layer. For example, in a fiber reinforced composite, it is typical to place the 1 direction along the fibers and the 2 direction perpendicular to the fibers. Qij are the reduced stiffness coefficients and can be written in terms of the material moduli E_1, E_2, G_{12} and Poisson's ratio ν_{12}.

$$Q_{11} = \frac{E_1}{1-\nu_{12}\nu_{21}};\ Q_{22} = \frac{E_2}{1-\nu_{12}\nu_{21}}$$
$$Q_{12} = \frac{\nu_{12}E_2}{1-\nu_{12}\nu_{21}};\ Q_{66} = G_{12} \quad (2)$$

For isotropic materials, as is the case for typical layered MEMS structures,

$$E_1 = E_2;\ \nu_{12} = \nu_{21};\ G_{12} = \frac{E}{2(1-\nu)} \qquad (3)$$

Thus only two material constants are required to define the mechanical properties of each layer. In CLPT, the stiffness matrix **Q** is rotated to align with the principal axes of the layered plate (x-y plane in Figure 1). This rotated stiffness matrix is referred to as $\overline{Q}$. For isotropic materials, the material properties are direction independent and no rotation is required (thus, $Q = \overline{Q}$).

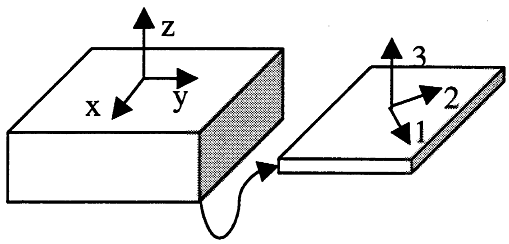

Figure 1: Schematic of a layered material with relevant coordinate axes.

Since either the loads or deformation are defined for the entire layered structure, it is important to define a "stress-strain" relationship for the laminate. The derivation begins with considering the strains in each layer with respect to the global xyz coordinate system. The deformation of the nth layer is related to the midplane strain ε_0 and curvature κ of the laminate:

$$\begin{Bmatrix} \varepsilon_x \\ \varepsilon_y \\ \gamma_{xy} \end{Bmatrix}_n = \begin{Bmatrix} \varepsilon_x \\ \varepsilon_y \\ \gamma_{xy} \end{Bmatrix}_0 + z_n \begin{Bmatrix} \kappa_x \\ \kappa_y \\ \kappa_{xy} \end{Bmatrix} \qquad (4)$$

where z_n is the distance of the nth layer from the midplane. z_n will be negative for layers located below the midplane. In this strain formulation there are several key assumptions: (i) each layer is linear elastic; (ii) there is no slip between the lamina interfaces, and (iii) a straight line in the z direction does not change in length and remains perpendicular to the laminate midplane.

The stress in each layer is determined by multiplying the strain in each layer by the layer stiffness matrix $\overline{Q}$:

$$\begin{Bmatrix} \sigma_x \\ \sigma_y \\ \tau_{xy} \end{Bmatrix}_n = \begin{bmatrix} \overline{Q}_{11} & \overline{Q}_{12} & \overline{Q}_{16} \\ \overline{Q}_{12} & \overline{Q}_{22} & \overline{Q}_{26} \\ \overline{Q}_{16} & \overline{Q}_{26} & \overline{Q}_{66} \end{bmatrix}_n \begin{Bmatrix} \varepsilon_x \\ \varepsilon_y \\ \gamma_{xy} \end{Bmatrix}_0 + z_n \begin{bmatrix} & & \\ & \overline{Q} & \\ & & \end{bmatrix}_n \begin{Bmatrix} \kappa_x \\ \kappa_y \\ \kappa_{xy} \end{Bmatrix} \qquad (5)$$

The strains and curvature in equations (4) and (5) correspond to those for the entire laminate.

A relationship between the loads imposed on the laminate and the laminate strain and curvature can be found by integrating the individual layer stresses over the thickness of the material. As is customary in CLPT, the load vector **N** and bending moment vector **M** are calculated per unit width, such that the units for **N** are N/m and for **M** are N. The three components for **N** correspond to the loads on the x and y faces with N_{xy} being the shear load on either the x or y face. A similar relationship holds for components of **M**.

Upon integration, a 6x6 matrix is formulated which relates the loads and bending moments applied to the laminate to the laminate deformation:

$$\begin{Bmatrix} N \\ M \end{Bmatrix} = \begin{bmatrix} A & B \\ B & D \end{bmatrix} \begin{Bmatrix} \varepsilon \\ \kappa \end{Bmatrix} \qquad (6)$$

A, **B**, and **D** are 3x3 matrixes that can be constructed from individual layer properties:

$$A_{ij} = \sum_{k=1}^{n} \left(\overline{Q}_{ij}\right)_k \left(h_k - h_{k-1}\right) \qquad (7)$$

$$B_{ij} = \frac{1}{2} \sum_{k=1}^{n} \left(\overline{Q}_{ij}\right)_k \left(h_k^2 - h_{k-1}^2\right) \qquad (8)$$

$$D_{ij} = \frac{1}{3} \sum_{k=1}^{n} \left(\overline{Q}_{ij}\right)_k \left(h_k^3 - h_{k-1}^3\right) \qquad (9)$$

In designing MEMS structures, the most common form of "loading" will occur as thermal loads. As will be shown, even the loading associated with piezoelectric actuation can be modeled as a thermal load. In a thermal load, strain is applied to the structure by applying a change in temperature. For an individual layer, the strain is a function of the coefficient of thermal expansion α (which can be axis dependent) and the change in temperature ΔT. The individual layer strains are combined to create an in plane load and moment vector for the laminate. The components for the in plane load vector are:

$$N_m^T = \Delta T \sum_{k=1}^{n} \overline{Q}_{ij}\Big|_k \alpha_j (h_k - h_{k-1}) \quad \text{m = x, y, xy} \quad \text{i = 1,2,6} \qquad (10)$$

Similarly, the components for the moment vector are:

$$M_l^T = \frac{1}{2} \Delta T \sum_{k=1}^{n} \overline{Q}_{ij}\Big|_k \alpha_j (h_k^2 - h_{k-1}^2) \quad \text{l = x,y,xy;} \quad \text{i = 1,2,6} \qquad (11)$$

Given this thermal load vector, a laminate midplane strain and curvature can be calculated following equation (6).

Equation (6) is the basis for calculating the deformation of a layered structure given the loads or visa versa. Although the formulation appears complex, the fundamental relationships can be programmed into a spreadsheet. There are also commercially available laminated plate codes that are included as part of text books on composite materials [4].

3 RESULTS

In this section, a case study in which predictions from laminated plate theory for the deflection of a PZT-actuated microbeam is compared with experimental data. A PZT actuated microplate fixed at both ends (hereafter referred to as a bridge), was designed and fabricated. The layer sequence and thickness is summarized in figure 2. The overall dimensions of the beam are 300 μm x 1000 μm x 2.675 μm. The beam was actuated by applying a voltage across the two PZT layers. Maximum beam deflection, at the center, was recorded using a high powered microscope. Note, these measurements are static measurements; the beam was not oscillated.

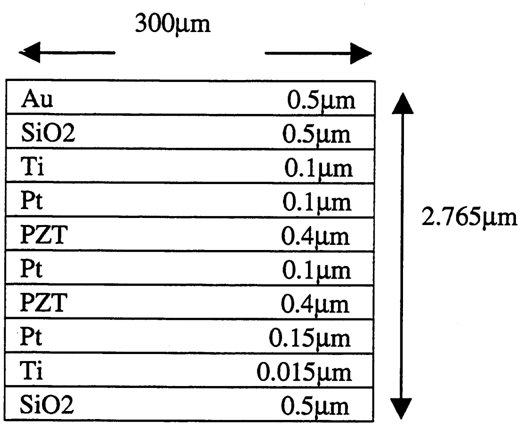

Figure 2: PZT actuated microbridge layer sequencing.

The actuated beam was modeled by CLPT. The strain in the PZT creates a "pseudo" thermal load in the PZT layer:

$$\varepsilon_x\Big|_{PZT} = \varepsilon_y\Big|_{PZT} = \frac{d_{31}}{t}V \qquad (12)$$

where t is the layer thickness, V is the applied voltage and d_{31} is the piezoresistive coupling coefficient between the 3 and 1 direction (which in this case are the same as the x and z directions respectively). The piezoelectric strain has a form similar to the thermal strain caused by a change in temperature. That is, the ratio d_{31}/t is substituted for the coefficient of thermal expansion α and V is substituted for ΔT. The coefficients of thermal expansion for all non-PZT layers are set to zero. Through this input format, commercial CLPT codes can be applied to study deformation in layered MEMS structures. A summary of material input data for each layer is shown in Table 1. Thin film properties (including PZT) were obtained from the literature [5]. The piezoresistive coupling component was -171 pC/N.

	E (GPa)	ν
Au	75	0.42
SiO_2	60	0.3
Ti	120	0.3
Pt	170	0.3
PZT	120	0.28

Table 1: Material properties for layers

The model predicted that the in-plane strain ($\varepsilon = \varepsilon_x = \varepsilon_y$) is 1.43E-4 per Volt applied, and the curvature($\kappa = \kappa_x = \kappa_y$) is 1.2E-5/m per Volt applied. Because the beam is fixed at both ends, a tensile in-plane strain ε will cause the beam to buckle. The fixed ends of the microbeam will limit the curvature caused by buckling κ_B:

$$\kappa_B = \frac{2\theta}{l_0(1+\varepsilon)} \qquad (13)$$

where l_0 is the length of the undeformed beam and θ is the angle associated with the curved beam (Figure 3):

$$\frac{\sin(\theta)}{\theta} = \frac{1}{1+\varepsilon} \qquad (14)$$

The deflection associated with the beam buckling curvature κ_B, as well as the deflection associated with the thermal curvature will contribute to the total displacement at the center of the beam [6]:

$$\delta = \frac{(\kappa_B + \kappa)l_0^{\,2}}{8} \qquad (15)$$

Figure 4 shows a comparison of model prediction and data for displacement of the microbeam.

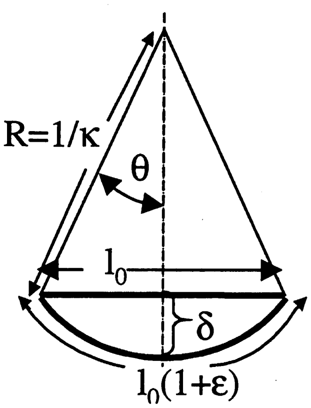

Figure 3: Schematic showing curvature of the beam caused by elongation at the midplane.

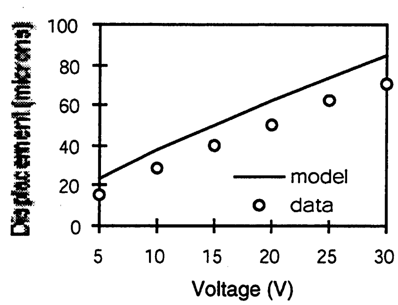

Figure 4: A comparison of model prediction and data for displacement of the microbeam.

Comparison between the model and experimental data is quite good. The model over-predicts the experimental data by 15%. Over-prediction in this case makes sense for several reasons. The model assumes simply supported boundary conditions and therefore overpredicts displacement. This result is as expected since the actual device boundary conditions lie in-between fixed-fixed and simply supported. In addition the coupling coefficient for thin film PZT is expected to be less than that published in the literature for bulk PZT. This case study illustrates the application of laminated plate theory to mechanical analysis of layered MEMS structures.

A similar approach has been used to calculate residual stresses and strains created during manufacture of layered beams. In this study of residual stresses, laminated plate theory predicts whether residual stresses created during fabrication will cause the beam to fail. Other potential applications include magnetically actuated structures. For these cases, the magnetic field can be approximated as a distributed load on the MEMS structure.

4 CONCLUSIONS

CLPT can be applied to layered MEMS structures to predict mechanical performance. Individual layer mechanical properties (including thermal expansion coefficients) are combined to create an overall stiffness matrix that combines the layered structure response to in plane and bending loads. This matrix formulation relates external loads applied to the layered structure and the structure midplane strain and curvature. From the overall laminate response, individual layer stresses and strains can be determined. A case study was presented in which deflection of a PZT actuated microbeam was predicted with CLPT.

REFERENCES

[1] DeVoe, D. L., and Pisano, A. P. (1997). "Modeling and Optimal Design of Piezoelectric Cantilever Microactuators." *Journal of Microelectromechanical Systems*, 6(3), 266-270.

[2] Vairac, P., Ballandras, S., and Cretin, B. (2001). "Finite Element Analysis of the Behavior of the Scanning Microdeformation Microscope." *IEEE Transactions on Ultrasonics, Ferroelectrics, and Frequency Control*, 48(4), 895-899.

[3] Kaw, A. K. (1997). *Mechanics of Composite Materials*, CRC Press, New York.

[4] Tsai, S. (1987). *Composites Design*, Think Composites, Dayton.

[5] Weinberg, M. (1999). "Working Equations for Piezoelectric Actuators and Sensors." *ASME/IEEE Journal of MEMS*, 8(4), 529-533.

[6] Roark, R. J., and Young, W. (1975). *Formulas for Stress and Strain*, McGraw-Hill Book Co., New York.

ACKNOWLEDGEMENTS

This work was supported by grant number DMII-9978744 from the National Science Foundation.